JOURNAL OF Applied Polymer SCIENCE

Special Issue: Manufacturing of Advanced Biodegradable Polymeric Components

Guest Editors: Prof. Roberto Pantani (University of Salerno) and
Prof. Lih-Sheng Turng (University of Wisconsin–Madison)

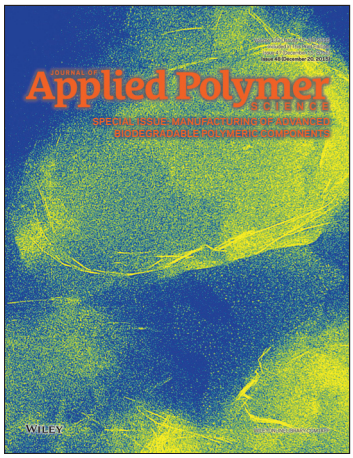

EDITORIAL

REVIEWS

ARTICLES

JOURNAL OF Applied Polymer SCIENCE

Special Issue: Manufacturing of Advanced Biodegradable Polymeric Components

Guest Editors: Prof. Roberto Pantani (University of Salerno) and Prof. Lih-Sheng Turng (University of Wisconsin–Madison)

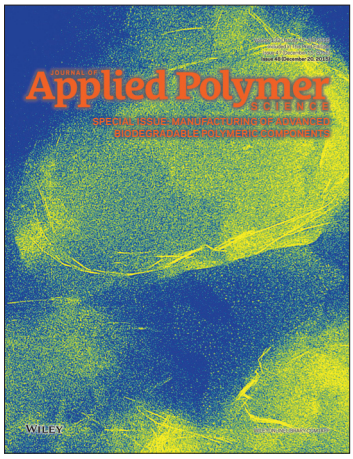

Rotational molding of biodegradable composites obtained with PLA reinforced by the wooden backbone of opuntia ficus indica cladodes
A. Greco and A. Maffezzoli, *J. Appl. Polym. Sci.* 2015, **DOI:** 10.1002/app.42447

Foam injection molding of poly(lactic) acid: Effect of back pressure on morphology and mechanical properties
V. Volpe and R. Pantani, *J. Appl. Polym. Sci.* 2015, **DOI:** 10.1002/app.42612

Modification and extrusion coating of polylactic acid films
H.-Y. Cheng, Y.-J. Yang, S.-C. Li, J.-Y. Hong and G.-W. Jang, *J. Appl. Polym. Sci.* 2015, **DOI:** 10.1002/app.42472

Processing and properties of biodegradable compounds based on aliphatic polyesters
M. R. Nobile, P. Cerruti, M. Malinconico and R. Pantani, *J. Appl. Polym. Sci.* 2015, **DOI:** 10.1002/app.42481

Journal of Applied Polymer Science

Largely toughening biodegradable poly(lactic acid)/thermoplastic polyurethane blends by adding MDI

Fei Zhao, Han-Xiong Huang, Shui-Dong Zhang
Laboratory for Micro Molding and Polymer Rheology, Department of Industrial Equipment and Control Engineering, The Key Laboratory of Polymer Processing Engineering of the Ministry of Education, South China University of Technology, Guangzhou 510640, People's Republic of China
Correspondence to: H.-X. Huang (E-mail: mmhuang@scut.edu.cn)

ABSTRACT: This work focuses on largely toughening poly(lactic acid)/thermoplastic polyurethane (PLA/TPU) blend with lower content (20 wt %) of TPU using appropriate contents of 4,4-methylene diphenyl diisocyanate (MDI) via simple melt blending. Both scanning electron micrographs and differential scanning calorimetry curves suggest little change of the compatibility between the PLA and TPU phases by adding the MDI. Dynamic rheological test demonstrates that a reaction occurs between the TPU phase and MDI during melt blending. Combining the rheological behaviors and gel contents of the blends, it can be speculated that adding the MDI extends the TPU chains and forms branched and crosslinked structure in the TPU chains sequentially. Toughening mechanism is analyzed and different impact strengths for the blends with different MDI contents are explained based on combined effects of the decreased crystallinities for the PLA matrix and the extended, branched and crosslinked structure in the TPU chains. A 0.8 wt % MDI content is optimal in terms of the impact strength (100.6 kJ/m^2) and the elongation at break (392.4%). The former is about 1.9 and 32.5 times of that for the blend without MDI and the PLA, respectively. Moreover, the MDI results in some increase in the tensile strength of the blends. © 2015 Wiley Periodicals, Inc. J. Appl. Polym. Sci. **2015**, *132*, 42511.

KEYWORDS: biodegradable; biopolymers and renewable polymers; blends; extrusion; polyurethanes

Received 29 November 2014; accepted 18 May 2015
DOI: 10.1002/app.42511

INTRODUCTION

Biopolymers have been attracted much attention from both industry and academia in recent years due to daily increased environmental concerns and continuously reduced amount of petroleum resources. Poly(lactic acid) (PLA), an aliphatic polyester derived from 100% renewable resources such as corn and sugar beets, is highly versatile and biodegradable.[1] PLA offers a wide range of applications, such as packaging, textile, and automotive industries, as a very promising ecofriendly alternative to traditional petroleum-based commodity polymers. Despite its numerous advantages such as high strength and stiffness and good optical, physical, and barrier properties, its low flexibility (elongation at break), and impact strength significantly impede its applications.[2] Therefore, blending PLA with flexible and biodegradable polymers, such as poly(ε-caprolactone) (PCL),[3,4] poly(butylene adipate-*co*-terephthalate),[5,6] and poly(butylene succinate),[7,8] is an effective way to toughen PLA. Thermoplastic polyurethane (TPU) elastomer is a block copolymer consisting of aromatic or aliphatic polyurethane "hard segments" and aliphatic polyester or polyether "soft segments". TPU has a unique combination of toughness, durability, flexibility, biocompatibility, and biostability that makes it suitable material for applications in a diverse range of implantable medical devices.[9,10] TPU has been used to successfully toughen PLA.[10–13] It was demonstrated that PLA/TPU blends exhibit remarkable increases in their impact strengths and elongations at break. Moreover, mechanical properties of PLA/TPU blends can be adjusted by changing TPU content. This can broaden the application range of PLA. More importantly, both PLA and TPU have good biocompatibility and so their blends can be used in biomedical applications.

Previous researches, however, demonstrated that the tensile strengths of PLA/TPU blends decrease with increasing TPU content due to lower yield strengths of TPU and weaker interactions between PLA and TPU phases.[10–13] TPU modification[14] is one of strategies for not only achieving superior toughing effect but also avoiding significant loss in tensile strengths for PLA/TPU blends. Very recently, chemicals containing diisocyanate groups were used for situ reactive compatibilization in preparing PLA/TPU blends.[15,16] Liu *et al.*[15] used crosslinked polyurethane (CPU) that was formed by *in situ* polymerization of polyethylene glycol and polymeric methylene diphenylene

diisocyanate to successfully toughen PLA. The compatibility between the PLA and TPU phases increases with increasing soft segment length and CPU content. Dogan *et al.*[16] used 1,4 phenylene diisocyanate (PDI) to improve the compatibility of PLA and TPU phases and so decrease the dispersed TPU phase size. Addition of the PDI results in large increases in the tensile strengths of the PLA/TPU (50/50) blends comparing with the blend without the PDI. Unfortunately, the impact strengths of the PLA/TPU blends were not investigated in their work. Among chemicals containing diisocyanate groups, 4,4-methylene diphenyl diisocyanate (MDI) is widely used for synthesizing TPU,[17,18] modifying PLA,[19] and preparing PLA/starch blends,[20] and PLA-based composites.[21,22] To the best knowledge of the authors, not much report has been published on the application of MDI in preparing PLA/TPU blends. Moreover, not much work has been conducted on toughened PLA systems with good toughness–strength balance using lower contents of elastomers.

For the aforementioned reasons, this work focused on PLA/TPU blend containing a lower content of TPU (20 wt %). The PLA/TPU (80/20) blend is expected to exhibit a little enhanced toughness especially impact strength. Hence, MDI was tried to add into the blend for simultaneously improving its toughness and strength. The effect of the MDI content on the properties of the PLA/TPU blends, including mechanical, thermal, and rheological properties, was investigated. Different impact strengths for the blends with different MDI contents are explained based on combined effects of the decreased crystallinities for PLA matrix and the extended, branched and crosslinked structure in TPU chains.

EXPERIMENTAL

Materials and Sample Preparation

The polymers used in this work were commercial PLA (grade 4032D, NatureWorks, USA) and polyester-based TPU (grade WHT-1185, Yantai Wanhua Polyurethanes, China). The PLA has a D-isomer content of 1.2–1.6% and a density of 1.24 g/cm^3. The TPU has a density of 1.2 g/cm^3. MDI, produced by Aladdin Industrial Corporation, China, has a melting point of 38–42°C and a boiling point of 200°C at 7 hPa.

Both PLA and TPU were dried in a vacuum oven at 80°C for 24 h. Then dried PLA and TPU as well as the MDI were dry-mixed thoroughly and directly fed into a single screw extruder with a diameter of 45 mm for melt blending. The extruder was equipped with a convective screw, which was demonstrated to induce dispersive melting and chaotic mixing.[23–25] The feed rate and screw speed were set at 4 kg/h and 40 rpm, respectively. The barrel temperatures were set at 140, 170, 180, and 180°C in order. The ratio of the PLA to TPU in the blends was fixed at 80/20 by weight. The blend samples with addition of 0, 0.2, 0.4, 0.8, 1.2, and 1.6 wt % MDI were denoted as PT-0, PT-0.2, PT-0.4, PT-0.8, PT-1.2, and PT-1.6, respectively. The molten blends were collected from the die exit and immediately compression molded into impact and tensile test samples at 20 MPa for 2 min. Moreover, the collected molten blends were quickly quenched in iced water to keep their original phase morphology for morphology observation and rheological tests. The samples for the rheological tests had a thickness of ~1.5 mm and a diameter of 25 mm. For comparison, neat PLA and TPU samples were also prepared via the extruder at the same processing conditions.

Tests and Characterization

Tensile tests were carried out using an Instron Universal Tester (5566, Instron Corp.) with a crosshead speed of 20 mm/min at room temperature. The notched impact tests were performed using a pendulum impact tester (PIT501B-Z, Shenzhen Wan Testing Lab Equipment). Five samples were used in each mechanical test and the average value was calculated.

The blend samples were immersed in liquid nitrogen for 20 min and cryofractured along the extrusion direction. The fractured samples were sputtered with gold and the fractured surfaces were observed on a scanning electron microscope (SEM, FEI Quanta 200). The mean diameter of a single droplet was calculated by averaging all of the diameters obtained from a rotation of 5° one time with the droplet centroid as the center. The mean droplet diameter (d) was calculated using the following equation:

$$\ln d = \frac{\sum_{i=1}^{N} n_i \ln d_i}{\sum_{i=1}^{N} n_i} \quad (1)$$

where d_i is the number of droplets with diameter of d_i in the SEM micrographs, N is the number of all of the droplets in the SEM micrographs.

Differential scanning calorimetry (DSC) measurements were performed using a differential scanning calorimeter (Netzsch 204C) under a nitrogen atmosphere. The specimens with about 5 mg, which were sliced from the tensile test samples, were heated from room temperature to 200°C at a heating rate of 3°C/min and held there for 3 min to erase any thermal history. Then, the specimens were cooled to −100°C with a cooling rate of 3°C/min and again heated to 200°C with a heating rate of 3°C/min. The crystallinity of PLA in the blends (X_c) was estimated according to the following equation:

$$X_c = \frac{\Delta H_m - \Delta H_{cc}}{W_f \Delta H_m^0} \times 100\% \quad (2)$$

where ΔH_m and ΔH_{cc} are the enthalpies of melting and cold crystallization during heating, respectively; ΔH_m^0 is the melting enthalpy of 100% crystalline PLA (93.7 J/g);[26] and W_f is the weight fraction of PLA component in the blends.

Fourier transform infrared spectroscopy (FTIR) analysis and gel fraction measurement were conducted on specimens with about 0.3 g, which were cut from the tensile test samples. The PT-0 and 0.8 specimens were put into fabric bags and extracted in Soxhlet extractor with boiling chloroform for 24 h, respectively. FTIR spectra were recorded for the resulting solution (PLA phase) and dried residue (TPU phase) on a Vector 3 spectrometer (Bruker) in a range of wavenumbers from 4000 to 400 cm^{-1}. The resolution and scanning time were 4 cm^{-1} and 32, respectively. For the gel fraction measurement, each specimen was put into a fabric bag and extracted in Soxhlet extractor with an excess volume of boiling oxolane for 24 h. Then the

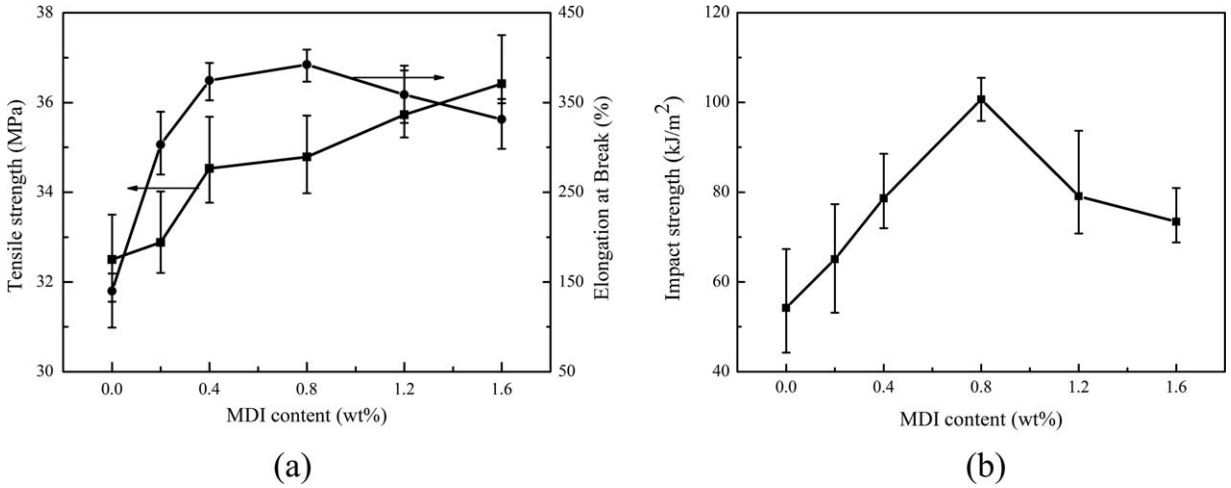

Figure 1. (a) Tensile strengths, elongations at break and (b) impact strengths vs. MDI content curves for prepared PLA/TPU blend samples.

extracted specimens with fabric bags were vacuum-dried to a constant weight after cleaned by the ethyl alcohol absolute and then water. According to the weight of the insoluble portion, the gel contents of the specimens were determined.

Rheological tests were performed on a rotational rheometer (Bohlin Gemini 200HR, Malven Instruments) with a parallel plate (diameter: 25 mm; gap: 1 mm). The rheological data were determined at a frequency range of 0.01–100 rad/s and a temperature of 180°C. A fixed strain of 1% was used to ensure that the tests were carried out within the linear viscoelastic range of the samples investigated.

RESULTS AND DISCUSSION

Mechanical Properties

The PLA sample is rigid and brittle with a tensile strength, elongation at break and impact strength of 46.2 MPa, 12.2% and 3.1 kJ/m^2, respectively. Figure 1 shows the tensile strengths, elongations at break, and impact strengths as a function of the MDI content for the prepared PLA/TPU blend samples. As can be seen, sample PT-0 exhibits an elongation at break of 139.8% and impact strength of 54.2 kJ/m^2. This indicates that a transition of the PLA from brittle to ductile fracture appears and the PT-0 shows a significant increase in toughness comparing with the PLA sample. However, the tensile strength of the PT-0 is reduced by about 30% comparing with the PLA sample. With the addition of the MDI, the elongations at break and the impact strengths of the PLA/TPU blends keep increasing until a MDI content of 0.8 wt % and then decrease. For sample PT-0.8, the elongation at break and the impact strength reach 392.4% and 100.6 kJ/m^2, respectively. The latter is about 1.9 and 32.5 times of that for samples PT-0 and PLA, respectively. To the best knowledge of the authors, relevant researches were carried out by Li *et al.*,[10] Han *et al.*,[11] Jaso *et al.*,[13] and Hong *et al.*,[27] for toughening PLAs using TPU via melt blending. Their results demonstrated that the impact strengths of PLA/TPU (80/20) blends are increased by only about 40–240% compared with those of corresponding PLAs. Moreover, the tensile strengths of the blend samples keep increasing with increasing MDI content [Figure 1(a)]. Therefore, the MDI greatly improves the toughness of the PLA/TPU blends with some increase in the tensile strength in this work.

Phase Morphology

To reveal the reason for the aforementioned toughness improvement of the prepared PLA/TPU blend samples due to the addition of the MDI, their phase morphologies are investigated. Figure 2 shows the SEM micrographs of cryofractured surfaces for the six blend samples. As shown in Figure 2(a), spherical TPU droplets with a relatively uniform size distribution are distributed in the PLA matrix for sample PT-0. The mean diameter of the dispersed TPU droplets calculated from eq. (1) is about 0.69 μm. Clearly, gaps between some TPU droplets and the PLA matrix appear on the fractured surfaces, as marked by circles. Moreover, many voids exist on the fractured surfaces, which are formed by pulling out the TPU droplets from the PLA matrix in the cryofracturing process. The voids and gaps mean poor compatibility between the PLA and TPU phases. As can be seen in Figure 2(b–f), the voids and gaps also appear on the fractured surfaces of the PLA/TPU blend samples with different MDI contents, which indicates little change for the compatibility between the two components with the addition of the MDI. The mean diameters of the dispersed TPU droplets are about 0.84, 0.99, 1.04, 1.05, and 1.04 μm for samples PT-0.2, PT-0.4, PT-0.8, PT-1.2, and PT-1.6, respectively; that is, the diameters of the TPU droplets are increased slightly with increasing MDI content, the reason for which will be analyzed later. Therefore, the improved toughness of the PLA/TPU blends with the addition of the MDI is uncorrelated with the compatibility of the PLA and TPU phases.

Thermal Properties

Compatibility in polymer blends can be judged by observing the shift in the glass transition temperature (T_g) of the phases in comparison to their original values, whereas the T_g values can be obtained by DSC measurement. So DSC measurements are performed to determine whether the compatibility between the PLA and TPU phases changes with the addition of the MDI

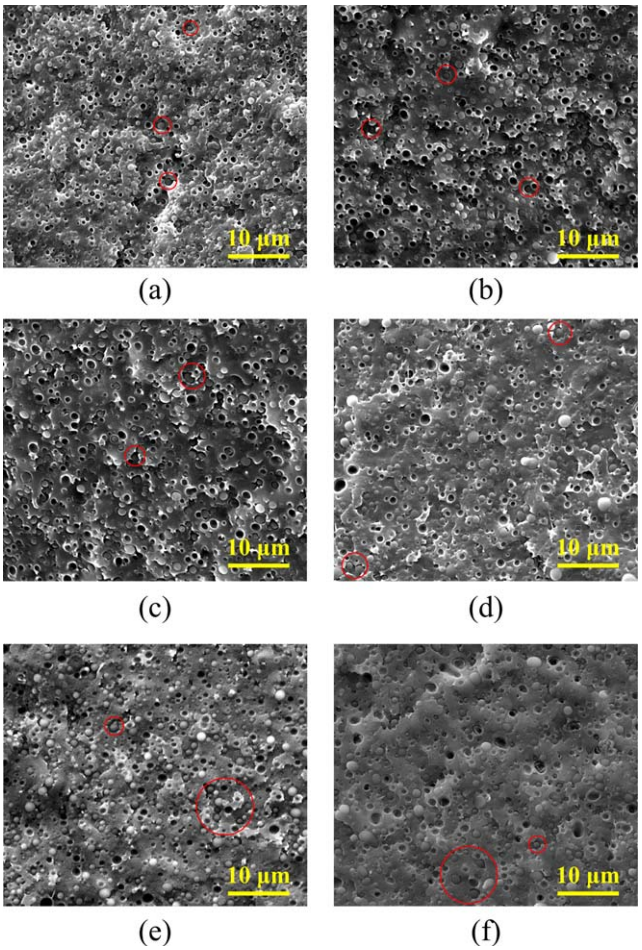

Figure 2. SEM micrographs of cryofractured surfaces for PLA/TPU blend samples with (a) 0, (b) 0.2, (c) 0.4, (d) 0.8, (e) 1.2, and (f) 1.6 wt % MDI. [Color figure can be viewed in the online issue, which is available at wileyonlinelibrary.com.]

in this section. Figure 3 shows the curves of the second heating run in the DSC measurements for four blend samples with different MDI contents. The thermal properties parameters obtained from the DSC curves, including T_g, crystallization temperature (T_c), lower melting temperature (T_{ml}), higher melting temperature (T_{mh}), and X_c, are summarized in Table I. As can be seen, with the addition of the MDI, the T_g values for the PLA and TPU phases in the PLA/TPU blend samples change little, which further confirms the aforementioned little change of the compatibility between the PLA and TPU phases with the addition of the MDI.

It can be seen in Figure 3 that the DSC curves for the four blend samples exhibit double-melting peaks. The double-

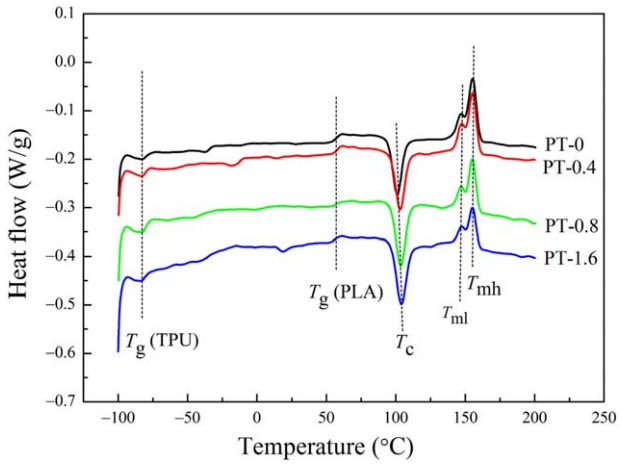

Figure 3. DSC thermograms of second heating run for four PLA/TPU blend samples with different MDI contents. [Color figure can be viewed in the online issue, which is available at wileyonlinelibrary.com.]

melting peaks were also found by some researchers for PLA and its blends.[20,28] For example, the research of Yu *et al.*[20] showed that double-melting peaks appear at the DSC curves for the PLA/cornstarch blends with the MDI added in, and it was explained by the melting recrystallization of the PLA phase. It is apparent in Table I that the T_{ml} and T_{mh} of the four blend samples are little affected by the addition of the MDI. Moreover, the T_c and X_c values for the blend samples are increased and decreased with increasing MDI content, respectively. It is speculated that this results from the reaction of the PLA or TPU phase with the MDI during melt blending in the extruder, which increases the molecular weight of the PLA or TPU phase and so retard or hinder the crystallization in the blend samples. Similar result was reported by Li *et al.*[29] on the research of biocomposites from PLA and distillers dried grains with solubles.

FTIR Spectroscopy

As mentioned above, the compatibility between the PLA and TPU phases changes little as the MDI added in, whereas the T_c shifts to higher values and the X_c keeps reducing with increasing MDI content for the PLA/TPU blend samples. Hence, the aforementioned toughness improvement for the blends is speculated to be attributed to a reaction of PLA or TPU phase with the MDI. To corroborate the reaction of the PLA or TPU phase with the MDI, the FTIR spectra (400–4000 cm^{-1}) for the PLA and TPU phases in samples PT-0 and PT-0.8 are presented in Figure 4. It can be seen that with the addition of the MDI, no new peaks appear at the FTIR spectra for both PLA and TPU phases. This implies that no reaction occurs between the PLA

Table I. Thermal Properties Parameters for four PLA/TPU Blend Samples with Different MDI Contents

Sample	T_g (PLA) (°C)	T_g (TPU) (°C)	T_c (°C)	T_{ml} (°C)	T_{mh} (°C)	X_c (%)
PT-0	56.6	−79.3	101.0	147.1	155.2	8.7
PT-0.4	57.4	−80.4	103.1	147.5	155.2	5.1
PT-0.8	56.9	−79.5	103.5	147.1	155.1	1.1
PT-1.6	56.3	−80.1	104.0	147.5	155.2	0.4

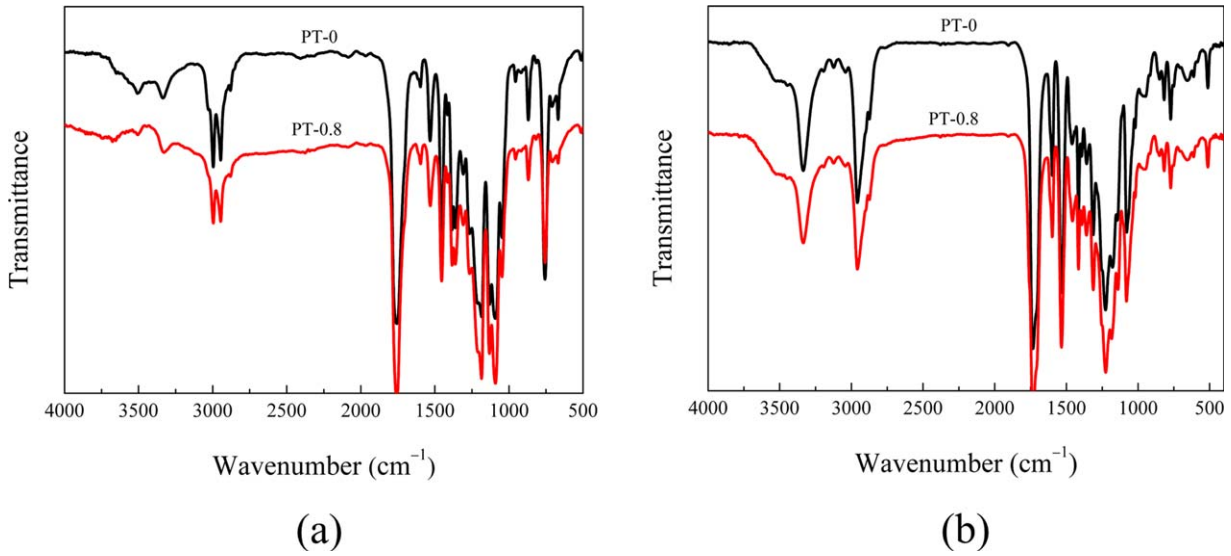

Figure 4. FTIR spectra for (a) PLA and (b) TPU phases in samples PT-0 and PT-0.8. [Color figure can be viewed in the online issue, which is available at wileyonlinelibrary.com.]

phase and MDI, which may be attributed to a small quantity of the terminal hydroxyl group of PLA. However, no reaction between the TPU phase and MDI cannot be confirmed because MDI may be used in TPU synthesization.[17,18]

Rheological Behavior

Rheological behavior of polymer is sensitive to change in its molecular structure. Therefore, it can be determined whether the reaction occurs and whether the PLA or TPU phase in the PLA/TPU blends reacts with the MDI by comparing the dynamic rheological behaviors of the PLA and TPU samples without and with the addition of the MDI in this work. Figure 5 illustrates the storage modulus (G') and complex viscosity (η^*) curves as a function of frequency (ω) for the extruded PLA and TPU samples without and with the addition of 0.8 wt % MDI tested at 180°C. As can be clearly seen, with the addition of the MDI, the values of the G' and η^* change little for the PLA sample and increase obviously for the TPU sample. This demonstrates that a reaction takes place between the TPU phase and MDI in the PLA/TPU blends.

The G' and η^* plotted as a function of ω for the six PLA/TPU blend samples with different MDI contents at 180°C are shown in Figure 6. As a whole, the G' and η^* of the blend samples keep increasing and more obvious shear-thinning behavior appears at lower frequency region with increasing MDI content. Specifically, both G' and η^* at lower frequency region exhibit obvious increases for the sample with 0.8 wt % MDI and further larger increases for the sample with 1.2 wt % MDI, whereas only a little further increases for the sample with 1.6 wt % MDI. The terminal slopes at G' vs. ω curves shown in Figure 6(a) for the blend samples are given in Table II. It is interesting to note that the terminal slopes are reduced for the blend samples with MDI contents of 0.8, 1.2, and 1.6 wt %.

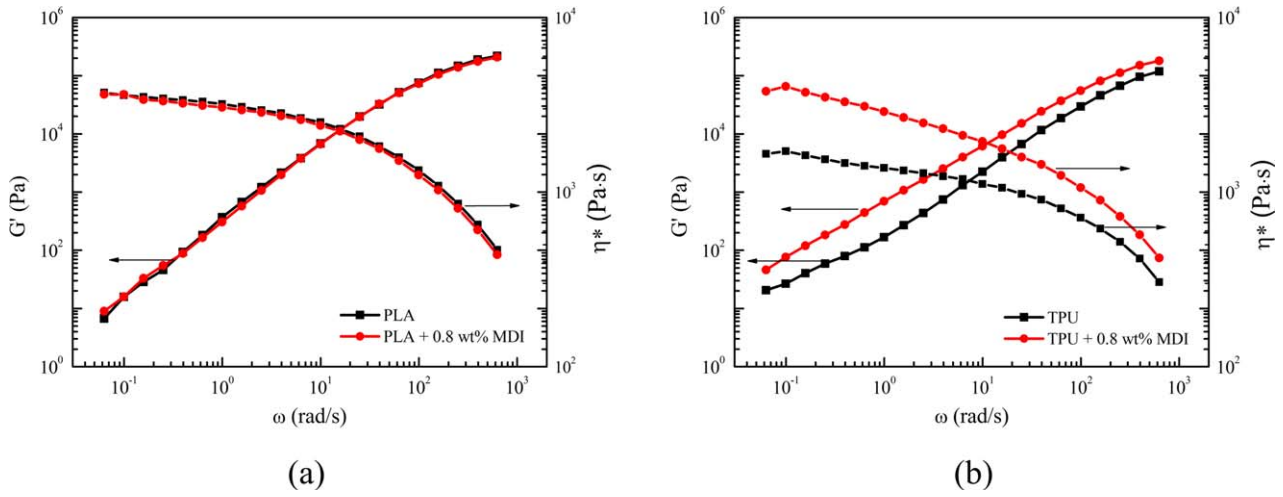

Figure 5. G' and η^* vs. ω curves for samples of (a) PLA and PLA with 0.8 wt % MDI and (b) TPU and TPU with 0.8 wt % MDI at 180°C. [Color figure can be viewed in the online issue, which is available at wileyonlinelibrary.com.]

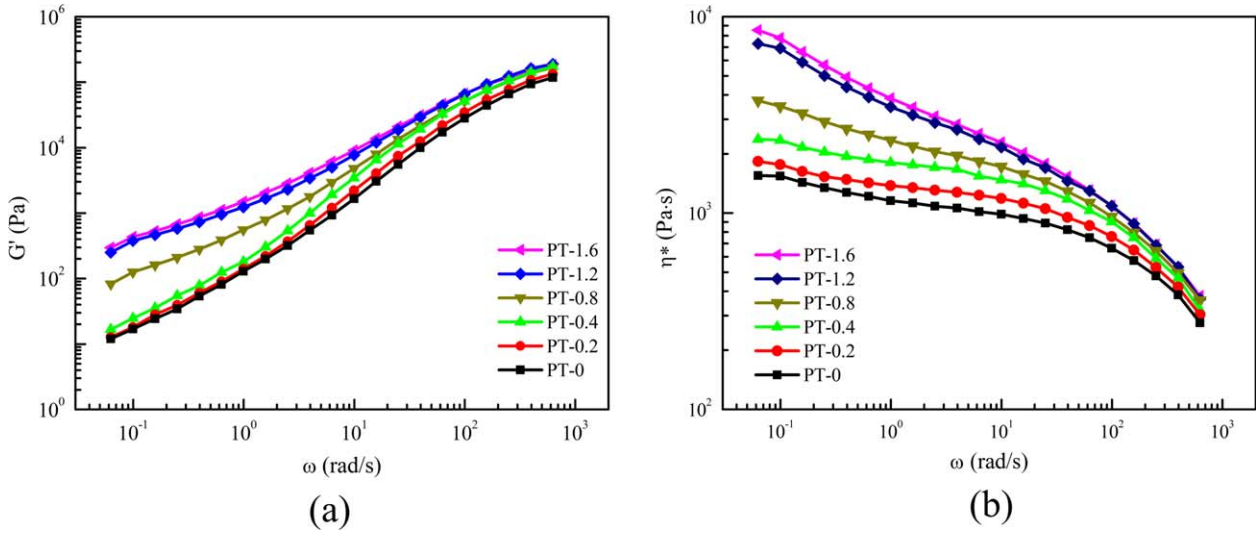

Figure 6. (a) G' vs. ω curves and (b) η^* vs. ω curves for six PLA/TPU blend samples with different MDI contents at 180°C. [Color figure can be viewed in the online issue, which is available at wileyonlinelibrary.com.]

Figure 7 gives the Cole–Cole plots for the six PLA/TPU blend samples tested at 180°C. It is evident from Figure 6 that two circular arcs appear at the plot for sample PT-0, which indicates that a second relaxation mechanism appears.[30] With the addition of the MDI, the arcs at the plots for the samples are broadened and shift up to higher viscosity region, indicating longer relaxation times. The upturning phenomenon at the plots appears at higher viscosity region for sample PT-0.8 and becomes more evident for samples PT-1.2 and PT-1.6. To quantitatively describe the relaxation times of the PLA/TPU blend samples, their critical frequencies (ω_c) are listed in Table III. The ω_c values are determined from the tan δ versus ω curves for the blend samples tested at 180°C, where the tan δ is obtained by dividing loss modulus (G'') by G'. The ω value corresponding to the point at the curve where the tan δ is equal to 1 is determined as the ω_c value. As shown in Table III, the ω_c values for the blend samples gradually decrease as the MDI content increases, which means increasing relaxation times for the blend samples with increasing MDI content.

Possible Reactions

The reaction between the TPU and MDI is confirmed in the above section. The research by Michell *et al.*[17] showed that the end diisocyanate groups in MDI can react with the hydroxyl groups in α,ω-dihydroxyl PLA macrodiol precursors and the amidogen groups in 4,4′-diaminodiphenylmethane (MDA) to form urethane groups in novel poly(ester-urethane)s. The reaction process in this work is schematically shown in Figure 8. First, the end diisocyanate groups of the MDI react with the end hydroxyl or amidogen groups of the TPU chains to form extended TPU chains. Then a reaction takes place between the end diisocyanate groups of the MDI and urethane groups in the extended TPU chains to form allophanate groups. The second less favorable reaction results in the formation of branched or crosslinked structure in the TPU chains. Depending on the aforementioned reaction process, the reaction extent can be controlled by changing the MDI content and so various PLA/TPU blends with different properties can be obtained.

The gel fraction measurement for the extruded six PLA/TPU blend samples demonstrates that samples PT-1.2 and PT-1.6 exhibit 2.1 and 2.3 wt % gel contents, respectively; whereas no gel is measured for other four samples. The aforementioned changes in the rheological behaviors of the PLA/TPU blend samples, including the increased G' and η^* (Figure 6), expanded relaxation arcs (Figure 7) and increased relaxation times (Table III) with increasing MDI content may be attributed to the reaction between the TPU and MDI. The decreased terminal slopes

Table II. Terminal Slopes at G' vs. ω Curves for Six PLA/TPU Blend Samples with Different MDI Contents

Sample	PT-0	PT-0.2	PT-0.4	PT-0.8	PT-1.2	PT-1.6
Terminal slope	0.77	0.78	0.85	0.66	0.59	0.58

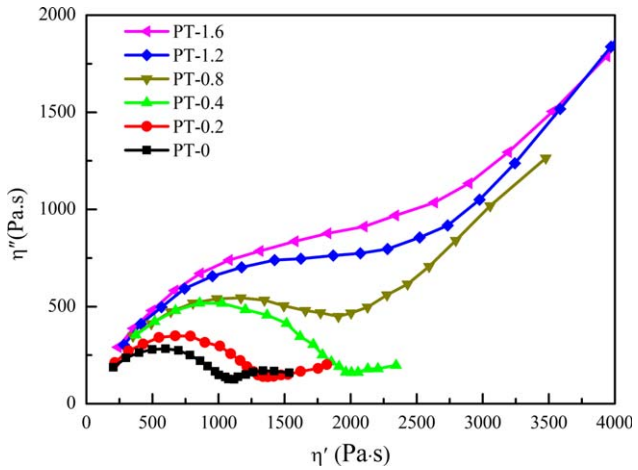

Figure 7. Cole–Cole plots for six PLA/TPU blend samples with different MDI contents at 180°C. [Color figure can be viewed in the online issue, which is available at wileyonlinelibrary.com.]

Table III. Critical Frequencies Determined from tan δ vs. ω Curves for PLA/TPU Blend Samples

Sample	PT-0	PT-0.2	PT-0.4	PT-0.8	PT-1.2	PT-1.6
ω_c (rad/s)	>628	>628	515	423	403	287

at the G' vs. ω curves (Table II), more obvious shear-thinning behavior at lower frequency region [Figure 6(b)] and upturning phenomenon at the Cole–Cole plots at higher viscosity region (Figure 7) may be attributed to generated branched chains or crosslinked structure in the TPU chains.[31,32] Now, combining the aforementioned rheological behaviors and gel contents, it can be speculated that adding the MDI extends the TPU chains and forms branched and crosslinked structure in the TPU chains sequentially. More specifically, with increasing MDI content, the TPU chains are extended (for samples PT-0.2 and PT-0.4), then branched TPU chains appear (for sample PT-0.8), and finally crosslinked structure also appears in the TPU chains (for samples PT-1.2 and PT-1.6). The aforementioned increased diameters of the dispersed TPU droplets from 0.69 to 1.05 μm with increasing MDI content can be explained by the increased melt viscosity of the TPU phase due to the generated chemical crosslinks between the TPU chains.

Toughening Mechanism Analysis

The toughening mechanism of the TPU in the PLA/TPU blends is analyzed as follows. The morphology around the central region of the Izod-impacted surfaces for both samples PT-0 and PT-0.8 is observed with SEM, and the results are shown in Figure 9. Crazing and shear yielding are known to be two main mechanisms of impact toughening in rubber-modified polymer blends at ambient temperature. Obvious phase separation that appears in Figure 9 indicates weak interactions between the TPU domains and PLA matrix. When the hydrostatic stresses are released, debonding is easily induced at the interfaces between the TPU domains and PLA matrix. The stresses elongate the TPU domains, the PLA matrix deforms more easily, then shear yielding occurs. This process dissipates a great deal of energy.[33] Moreover, as already demonstrated that an optimum domain size range exists for a rubber-toughened polymer system.[34,35] It was found by Bai *et al.*[36] that an optimum domain size range is 0.7–1.1 μm for toughening amorphous PLLA using PCL. In this work, the TPU domain diameters in the PLA/TPU blend samples with different MDI contents are in the range of 0.69–1.05 μm (Figure 2), which are all in the aforementioned range.

Further, different impact strengths for the PLA/TPU blend samples with different MDI contents (Figure 1b) are explained from the following three aspects. First, the X_c values for PLA matrix in the blends are decreased with increasing MDI content (Table I). The increased amorphous regions in the PLA matrix can improve its ability to absorb more energy. Second, extended especially branched structure formed in samples PT-0.2, 0.4, and 0.8 can strengthen the ability for the TPU domains to prevent cracks from propagating and triggering pervasive multiple crazing in the PLA matrix.[37] However, the generated chemical crosslinks between the TPU chains in samples PT-1.2 and 1.6 results in more hard segment in the TPU chains and so weaker ability to prevent cracks from propagating and triggering pervasive multiple crazing in the PLA matrix. This may lower the impact strengths for the two samples. So the combined effects of the decreased X_c values for the PLA matrix and the extended, branched and crosslinked structure in the TPU chains determine the impact strengths of the PLA/TPU blends with different MDI contents. Sample PT-0.8 exhibits the highest impact strength. Thirdly, it is evident from Figure 9 that compared with sample PT-0, the PLA matrix exhibits more obvious and extensive deformation and so coarse fibers are formed in PT-0.8, which means stronger ability to dissipate impact energy in impact tests. Moreover, the combined effects mentioned above also increases the tensile strengths of the PLA/TPU blends to some extent.

CONCLUSIONS

Biodegradable PLA/TPU (80/20) blends with addition of different contents of MDI were prepared using a single screw extruder specially designed by our laboratory. Compatibility between the PLA and TPU phases changes little by adding the MDI, which is confirmed by analyzing the phase morphology and the T_g values for the PLA and TPU phases in the PLA/TPU blends. A reaction takes place between the TPU phase and MDI during melt blending, which is confirmed by analyzing the dynamic rheological behaviors of the PLA and TPU without and with the addition of the MDI and the T_c values for the PLA/TPU blends. Further, possible reaction process is proposed by combining the rheological behaviors and gel contents of the PLA/TPU blends. That is, with increasing MDI content, the TPU chains are extended, then branched TPU chains appear,

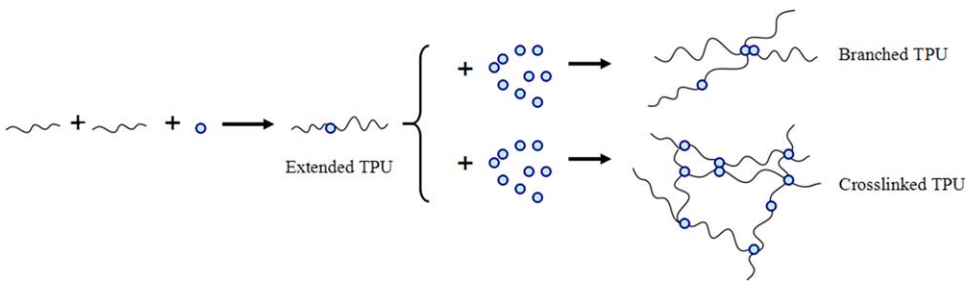

Figure 8. Schematic for reactions of TPU with MDI in this work. [Color figure can be viewed in the online issue, which is available at wileyonlinelibrary.com.]

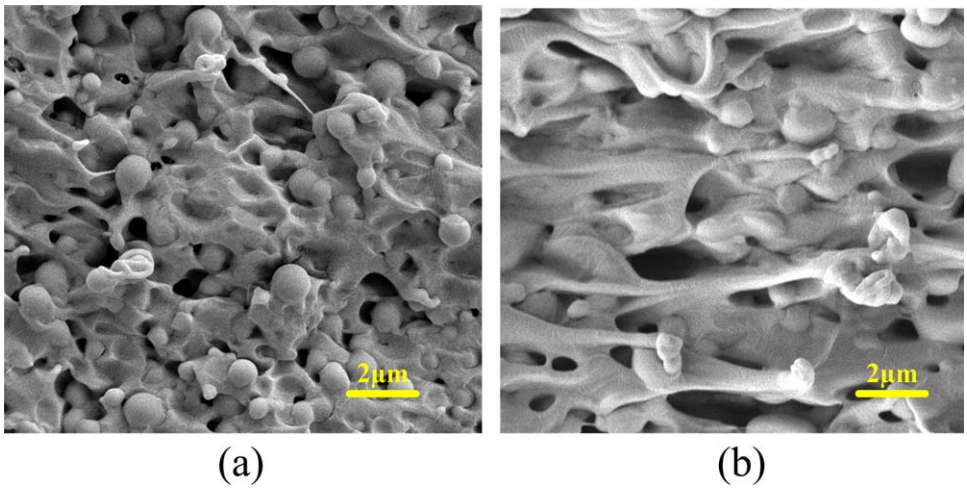

Figure 9. SEM micrographs taken from central region of Izod-impacted surface for samples PT-0 and PT-0.8. [Color figure can be viewed in the online issue, which is available at wileyonlinelibrary.com.]

and finally crosslinked structure also appears in the TPU chains. The impact strengths of the PLA/TPU blends are determined by combined effects of the decreased X_c values for the PLA matrix and the extended, branched and crosslinked structure in the TPU chains. The impact strength and the elongation at break for the blend with 0.8 wt % MDI reach 100.6 kJ/m^2 and 392.4%, respectively. The former is about 1.9 and 32.5 times of that for the blend without MDI and the PLA, respectively. Upon addition of the MDI, the PLA/TPU blends not only are largely toughened but also exhibit some increase in the tensile strength.

ACKNOWLEDGMENTS

Financial support provided by the National Natural Science Foundation of China (Grant No. 11172105) is gratefully acknowledged.

REFERENCES

1. Drumright, B. E.; Gruber, P. R.; Henton, D. E. *Adv. Mater.* **2000**, *12*, 1841.
2. Liu, H. Z.; Zhang, J. W. *J. Polym. Sci. Pt. B: Polym. Phys.* **2011**, *49*, 1051.
3. Sivalingam, G.; Vijayalakshmi, Madras, S. P. *Ind. Eng. Chem. Res.* **2004**, *43*, 7702.
4. López-Rodrguez, N.; López-Arraiza, A.; Meaurio, E.; Sarasua, J. R. *Polym. Eng. Sci.* **2006**, *46*, 1299.
5. Li, K.; Peng, J.; Turng, L.-S.; Huang, H. X. *Adv. Polym. Technol.* **2011**, *30*, 150.
6. Al-Itry, R.; Lamnawar, K.; Maazouz, A. *Rheol. Acta* **2014**, *53*, 501.
7. Wang, R. Y.; Wang, S. F.; Zhang, Y.; Wan, C. Y.; Ma, P. M. *Polym. Eng. Sci.* **2009**, *49*, 26.
8. Wu, D.; Yuan, L.; Laredo, E.; Zhang, M.; Zhou, W. *Ind. Eng. Chem. Res.* **2012**, *51*, 2290.
9. Stokes, K.; McVenes, R.; Anderson, J. M. *J. Biomater. Appl.* **1995**, *9*, 321.
10. Li, Y. J.; Shimizu, H. *Macromol. Biosci.* **2007**, *7*, 921.
11. Han, J. J.; Huang, H. X. *J. Appl. Polym. Sci.* **2011**, *120*, 3217.
12. Zeng, J. B.; Li, Y. D.; He, Y. S.; Li, S. L.; Wang, Y. Z. *Ind. Eng. Chem. Res.* **2011**, *50*, 6124.
13. Jaso, V.; Cvetinov, M.; Rakic, S.; Petrovic, Z. S. *J. Appl. Polym. Sci.* **2014**, *131*, #41104.
14. Lambour, P.; Mechin, F.; Pascault, J. P. *Polym. Eng. Sci.* **2002**, *42*, 68.
15. Liu, G. C.; He, Y. S.; Zeng, J. B.; Xu, Y.; Wang, Y. Z. *Polym. Chem.* **2014**, *5*, 2530.
16. Dogan, S. K.; Reyes, E. A.; Rastogi, S.; Ozkoc, G. *J. Appl. Polym. Sci.* **2014**, *131*, #40251.
17. Michell, R. M.; Müller, A. J.; Boschetti-de-Fierro, A.; Fierro, D.; Lison, V.; Raquez, J. M.; Dubois, P. *Polymer* **2012**, *53*, 5657.
18. Wu, J. A.; Ge, Q.; Mather, P. T. *Macromolecules* **2010**, *43*, 7637.
19. Li, B. H.; Yang, M. C. *Polym. Adv. Technol.* **2006**, *17*, 439.
20. Yu, L.; Petinakis, E.; Dean, K.; Liu, H. S.; Yuan, Q. *J. Appl. Polym. Sci.* **2011**, *119*, 2189.
21. Chen, F.; Liu, L. S.; Cooke, P. H.; Hicks, K. B.; Zhang, J. W. *Ind. Eng. Chem. Res.* **2008**, *47*, 8667.
22. Petinakis, E.; Long, Y.; Edward, G.; Dean, K.; Liu, H. S.; Scully, A. D. *J. Polym. Environ.* **2009**, *17*, 83.
23. Li, K.; Huang, H. X. *Polym. Eng. Sci.* **2012**, *52*, 2157.
24. Jiang, G.; Huang, H. X. *Polym. Eng. Sci.* **2011**, *51*, 2345.
25. Jiang, G.; Huang, H. X. *J. Mater. Sci.* **2008**, *43*, 5305.
26. Ojijo, V.; Ray, S. S.; Sadiku, R. *ACS Appl. Mater. Interfaces.* **2013**, *5*, 4266.
27. Hong, H.; Wei, J.; Yuan, Y.; Chen, F. P.; Wang, J.; Qu, X.; Liu, C. S. *J. Appl. Polym. Sci.* **2011**, *121*, 855.
28. Yasuniwa1, M.; Tsubakihara, S.; Sugimoto, Y.; Nakafuku, C. *J. Polym. Sci. Pt. B: Polym. Phys.* **2004**, *42*, 25.
29. Li, Y. H.; Sun, X. S. *J. Appl. Polym. Sci.* **2011**, *121*, 589.

30. Xu, L. Q.; Huang, H. X. *J. Appl. Polym. Sci.* **2012**, *125*, 272.
31. Su, F. H.; Huang, H. X. *Adv. Polym. Technol.* **2009**, *28*, 16.
32. Tian, J. H.; Yu, W.; Zhou, C. X. *Polymer* **2006**, *47*, 7962.
33. Wu, S. A. *J. Appl. Polym. Sci.* **1988**, *35*, 549.
34. Wu, S. *Polymer* **1985**, *26*, 1855.
35. Wu, S. *Polym. Eng. Sci.* **1990**, *30*, 753.
36. Bai, H. W.; Huang, C. M.; Xiu, H.; Gao, Y.; Zhang, Q.; Fu, Q. *Polymer* **2013**, *54*, 5257.
37. Geng, C. Z.; Su, J. J.; Han, S. J.; Wang, K.; Fu, Q. *Polymer* **2013**, *54*, 3392.